Curr Radiol Rep (2015) 3:4
DOI 10.1007/s40134-014-0084-6



# New Approaches to Reduce Radiation While Maintaining Image Quality in Multi-Detector-Computed Tomography

**Juan C. Ramirez-Giraldo · Matthew Fuld · Katharine Grant · Andrew N. Primak · Thomas Flohr**

Published online: 21 January 2015


**Abstract** This review discusses new technological approaches to reduce radiation dose while maintaining image quality in multi-detector-computed tomography (CT) for both adult and pediatric applications. First, the review focuses on the principles of automatic exposure control (AEC) systems for modulation of the tube current according to patient's size; as well as special AEC adaptations for cardiac CT and organ-based tube current modulation. The selection of the tube potential (kV) is also discussed, with particular emphasis in a new technology which allows an automatic selection of the tube potential with a corresponding adjustment in the tube current, according to patient's size and diagnostic task. The principles of iterative reconstruction, which is quickly becoming a standard feature in CT scanners, are also presented with particular emphasis on dose reduction and image quality. A full section is devoted to two latest state-of-the-art applications which can be used for radiation dose reduction: virtual non-contrast imaging with dual-energy CT and ultra-low dose CT with added spectral filtration. In the final section, innovations in CT hardware are presented ranging from the X-ray tube to CT detectors, which enable data acquisition at faster speeds and better efficiency to improve the balance between radiation dose and image quality.

**Keywords** Computed tomography · Radiation dose reduction · Radiation dose optimization · Image quality optimization · Iterative reconstruction · Dual-energy CT

## Introduction

A fundamental challenge in computed tomography (CT) is the balance between radiation exposure (dose) and image quality. The challenge lays in the fact that the lower the radiation dose used, the higher the image noise and the lower the image quality obtained. Hence, improvements in the selection of CT acquisition parameters, image reconstruction process, and CT hardware are needed to overcome this trade-off such that image quality can be maintained in spite of the use of lower radiation exposures. Importantly, a recent trend in CT technologies is the individualization of the CT examination to each patient by adapting the radiation dose according to patient size and/or age [1, 2]. The CT examination can also be adapted to different diagnostic tasks; for example, adapting the acquisition parameters according to whether or not iodinated contrast agent is needed [3]. However, individualizing CT scanning techniques to each individual patient and for various diagnostic tasks can be challenging to implement in a busy clinical practice, and difficult to manage if implemented manually. Asking radiologists and CT technologist to select a new set of parameters for each individual patient that comes in for a CT scan is not feasible. Fortunately, CT manufacturers are increasingly offering automated technologies to address the challenge of individualization. Three essential emerging technologies that allow tailoring

This article is part of Topical Collection on *Radiation Exposure and Reduction*.

J. C. Ramirez-Giraldo (✉) · M. Fuld · K. Grant · A. N. Primak
Siemens Medical Solutions USA Inc., 51 Valley Stream Parkway, Mail Code J29, Malvern, PA 19355, USA
e-mail: juancarlos.ramirezgiraldo@siemens.com

T. Flohr
Siemens Healthcare, Siemensstrasse 1, 91301 Forchheim, Germany

of the CT examination include automatic exposure control (AEC) of the tube current ("Automated exposure control of the tube current" section), optimal selection of the tube potential ("Radiation exposure adaptation by selecting the X-ray tube potential" section), and iterative reconstruction (IR) methods ("Iterative reconstruction" section). At the same time, new advanced CT applications ("Advanced CT acquisition modes in last generation CT scanners" section ) such as dual-energy CT and ultra-low dose imaging with added spectra filtration also offer opportunities to better tailor the examination to patients and exam types while at the same time reducing radiation dose. Finally, optimization of CT acquisition and new scanning modes are enabled by improvements in the CT hardware, especially in essential components such as the X-ray tubes and CT detectors ("Advances in CT scanner hardware components" section).

## Automated Exposure Control of the Tube Current

Changes in the X-ray tube current directly impact not only radiation dose but also affect the image noise. Reducing the tube current is desirable because it reduces the radiation exposure. However, the reduction of tube current, while keeping all other CT parameters the same, leads to an increase in image noise. Hence, to balance radiation dose and image noise, it is important to properly set up the tube current such that image noise is not excessively increased. One approach to find such a balance is to (manually) adapt a fixed tube current value to a CT examination according to some criteria, such as patient size or patient age [4]. For example, it is necessary to increase the tube current for large patients just as it is necessary to reduce the tube current for smaller patients. Adapting the tube current according to patient size (i.e., weight) is a first step to better balance radiation dose [4] and is advocated by various professional organizations such as the alliance for radiation safety in pediatric imaging (Image Gently®) [5], Image Wisely™ [6], or the Eurosafe Imaging [7]). Notably, all modern CT scanners now offer the possibility to automatically and continuously adapt the tube current to each individual patient size and anatomy, hence, in most cases obviating the need for detailed manual technique charts.

Tube current modulation is achieved with the use of AEC systems, which vary from one manufacturer to another. There are major advantages in using AEC systems: first, just like manual adaptation based on patient weight, AEC system can adapt the overall tube current according to the patient size [8]. Second, AEC systems can also modulate the tube current according to the patient's anatomy, such that it can maximize dose reduction potential while avoiding loss in image quality. This optimization of dose reduction while maintaining image quality can be achieved by continuously modulating the tube current angularly (i.e., in the $x$–$y$ plane) and also, in some cases, longitudinally (i.e., in the $z$-plane) (Fig. 1). The angular tube current modulation varies the tube current such that a higher value is applied laterally (where patients are typically thicker and hence more attenuating) relative to the value applied antero-posteriorly which is usually lower (where patients tend to be thinner and hence less attenuating). Similarly, the longitudinal adaptation of the tube current corresponds to changes along different anatomical locations. For example, the total attenuation path is usually shorter along the chest because the lungs are filled with air, while the total attenuation path increases in the abdomen and pelvis, where there is more mass that will attenuate the X-rays. The third benefit of AEC is that by better adapting the tube current, it is also possible to provide a more uniform image quality both across different patients and within individual patients.

The use of AEC has been reported to allow dose reductions up to 65 % when compared to approaches with fixed tube current while maintaining similar image quality. AEC has been proved useful both in adult [8–10] and pediatric examinations [11, 12]. Unfortunately, AEC systems become less effective with increasing longitudinal detector width, because the detector will then simultaneously cover anatomies with different attenuations (such as the lung and the liver), and the tube output can only be optimized for one of these anatomies.

The discussed AEC concepts are generally applicable to solutions offered by all manufacturers and in fact, AEC is currently considered a standard feature in modern CT scanners [13]. However, the actual implementation details across manufacturers have differences, most notably with the control variable that is used to adapt the tube current.

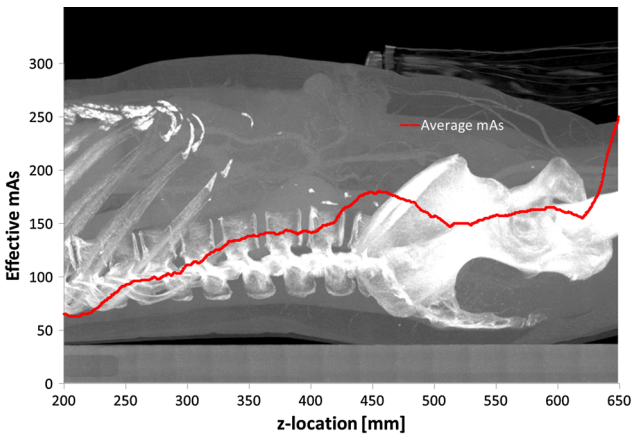


**Fig. 1** Continuous variation of the effective tube-current–time product (effective mAs) using Siemens CAREDose4D automatic exposure control

The most common control variables are the quality reference mAs, the reference image, and the standard deviation or noise index [14] (Table 1). For all cases, the user sets up the control variable to achieve the target image quality. For example, a quality reference mAs provides the desired image quality (i.e., image noise) if you were to scan a (reference) patient of approximately 75 kg. Likewise, one could define the desired image noise level (standard deviation or noise index) as the control variable, such that the AEC system will adapt the tube current up and down to achieve the target image quality according whether the attenuation is larger or smaller than the reference. Another important characteristic which is common to all AEC systems is the use of one or two CT localizer images (e.g., topograms) to estimate the patient's attenuation profile and hence to predict how the tube current is going to be modulated.

One implementation of AEC is CAREDose4D (Siemens Healthcare) in which the tube current automatically (and continuously) adapts to the size and shape of the patient both angularly and longitudinally (Fig. 2). In addition, CAREDose4D has a built-in 'real-time' feedback mechanism which further adapts the tube current based on the patient's attenuation profile obtained from the previous half rotation. This allows obtaining a more accurate estimate of the patient's attenuation compared to that from the localizer radiograph(s).

## Organ-Based Tube Current Modulation

Organ-based tube current modulation is a special type of AEC that aims to reduce dose to radiosensitive organs such as the breast, eye lens, or thyroid [15]. This reduction is achieved by decreasing the tube current over radiosensitive organs (Fig. 3). X-CARE (Siemens Healthcare, Forchheim, Germany) is an example of a technology designed for this purpose. X-CARE can decrease the tube current in a range of 120° (e.g., in the anterior surface of the organ such as the breast). Then, the tube current is increased for the X-ray projections corresponding to the remaining 240° to compensate for the lower photon count from the anterior projections that use only a fraction of the maximum tube current, such that the overall image quality is equivalent to that achieved with traditional AEC. To be able to balance the radiation dose of anterior and posterior projections, X-CARE requires a spiral pitch not larger than 0.6. We should note that conventional angular modulation does not work with X-CARE. However, just as a traditional AEC system, X-CARE adapts the tube current to patient size and is able to modulate the tube current longitudinally to accommodate for continuous changes in patient anatomy.

Various investigators have found that for equivalent scanner radiation output (i.e., equivalent $CTDI_{vol}$) X-CARE can reduce the exposure to the anterior surface by 17–50 % depending on anatomic region (head or thorax) and phantom size [15–17] without artifacts or significant changes in image noise. Other investigators have compared the effectiveness of organ-based tube current modulation with that of the bismuth shields and a global reduction of the tube current for the entire examination. For fixed radiation output, Wang et al. found that the eye lens dose reductions were comparable for X-CARE and bismuth shielding: 30 versus 26 %, respectively [18]. However, the image quality was preserved (noise and CT number accuracy) with X-CARE, while the image quality was deteriorated with the use of bismuth shields. In the same study, they also found that a global reduction of the tube current by 30 % resulted not only in a dose reduction of 30 % to the eye lens but also to all organs in the head, with a corresponding increase in noise (comparable to the bismuth shields), while maintaining CT number accuracy (as was possible with X-CARE). Similar findings were also reported in other studies of the thorax and neck in which organ-based tube current modulation led to reductions in superficial dose as with bismuth shields but with the advantage of maintained image quality [19]. In addition to the loss of image quality, other issues with bismuth shields have been reported, particularly when they are used in conjunction with systems that use AEC or placed in very close to the organs they mean to protect. There is a growing consensus that the use of a global reduction of the tube current or organ-based tube current modulation such as X-CARE should be preferred over the use of bismuth shields [20].

**Table 1** Automatic exposure control systems available by CT manufacturers

| Manufacturer[a] | Commercial name | Control variable |
|---|---|---|
| General Electric | SmartmA | Noise index |
| Hitachi | Intelli EC | Noise index |
| Neusoft | ACS+DOM | Reference image |
| Philips | 3D-DOM | Reference image |
| Siemens | CAREDose4D | Quality reference mAs |
| Toshiba | SURE Exposure 3D | Standard deviation |

[a] Listed in alphabetical order

## Automatic Exposure Control in Cardiac CT Examinations

A special modification of AEC algorithms is needed for cardiac CT. In cardiac CT, the tube current is modulated primarily as a function of the electrocardiographic (ECG) signal. There are two basic types of cardiac CT acquisition modes which are defined by how they manage the tube

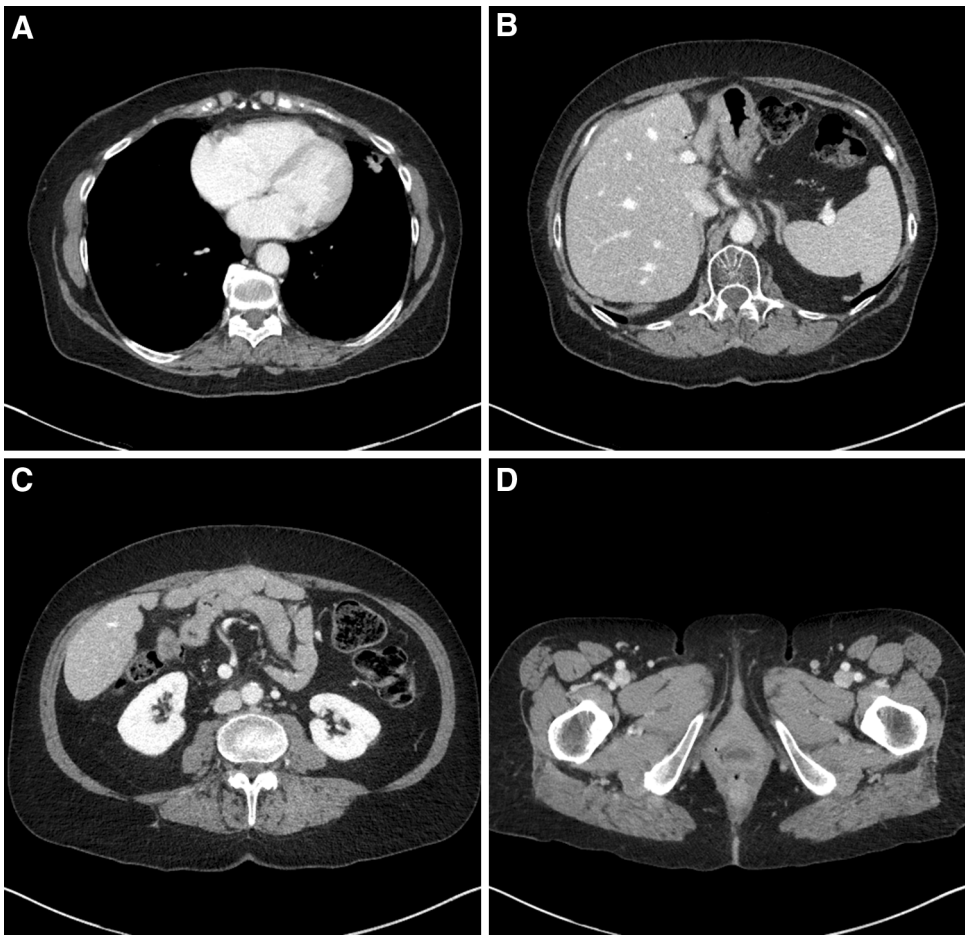


**Fig. 2** Continuous adaptation of the tube current with automated exposure control (AEC) using CAREDose4D, which was set up with 180 quality reference mAs. The actual effective mAs values applied to different positions along the patient varies as a function of the patient attenuation as illustrated in this example. **a** 65 mAs, **b** 111 mAs, **c** 165 mAs, and **d** 230 mAs

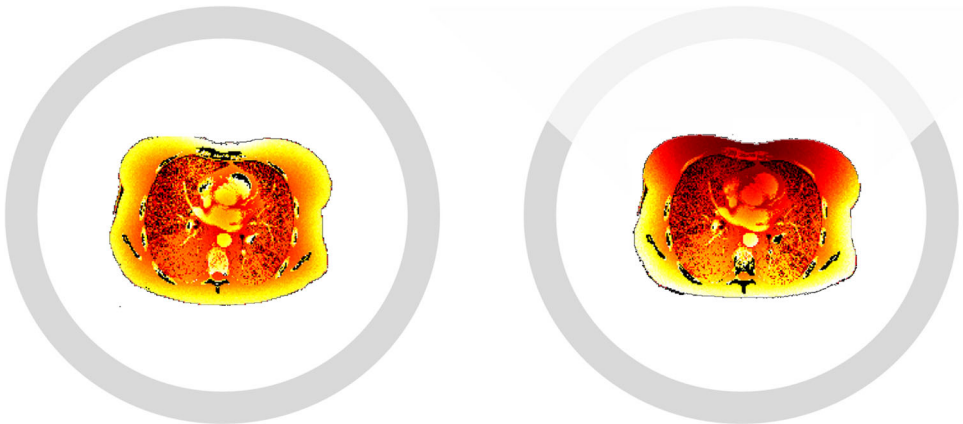

**Fig. 3** Organ-based tube current modulation with XCARE. Compared to routine tube-current modulation (*left*) the tube current is reduced in the anterior portion over a range of 120° (*right*). As a result, the radiation exposure to superficial radiosensitive organs such as the breast is reduced as depicted by the color-coded Monte Carlo simulation of the distribution of organ doses. *Darker color* indicates lower organ dose, and *brighter color* indicate a larger organ dose value

current modulation; the retrospectively ECG-gated spiral acquisition and the prospectively ECG-triggered sequential acquisition. In the retrospective mode, which typically uses a spiral pitch below 0.3, the tube current can be maintained at its maximum value throughout the entire examination providing similar image quality for all cardiac phases. A shortcoming of this approach is a high radiation exposure. Moreover, the information about the coronary anatomy

obtained from one cardiac phase is often sufficient for an accurate diagnosis. Therefore, the radiation dose during the retrospectively gated acquisition can be reduced by keeping the tube current at its maximum value only for a preselected cardiac phase (e.g., the best diastole or best systole) and reducing it to a lower value (e.g., 20 % of the maximum) outside of this preselected acquisition window. One example of this approach is the adaptive ECG-pulsing method (Siemens Healthcare) that provides ECG-controlled dose modulation for cardiac spiral CT. With the adaptive ECG-pulsing method, it is possible to reduce the tube current to a value as low as 4 % (MinDose$^{TM}$, Siemens Healthcare). This technology has been consistently reported to reduce the mean radiation dose by up to 30–50 % [21], leading to typical effective doses between 4 and 9 mSv [22].

In the prospectively ECG-triggered technique, the X-rays are only turned-on during the cardiac phase(s) of interest using a sequential (aka step-and-shoot) acquisition mode. This allows for further radiation dose reduction, when comparing to the retrospective technique. One example of this approach is the Adaptive Cardio-Flex-Sequence technique (Siemens Healthcare), in which the patient's ECG-signal is monitored during the examination, and axial scans are started with a pre-defined temporal offset relative to the R-waves. This mode of acquisition is a dose-efficient way of ECG-synchronized scanning because only the very minimum amount of data needed for image reconstruction is acquired during the preselected heart phase. A key advance with the Adaptive Cardio-Flex Sequence technique is that it can be used in patients with arrhythmia. Since the prospective technique depends on a reliable prediction of the patient's next cardiac cycle, the advanced algorithm employed by the Adaptive Cardio-Flex Sequence detects irregularities and in case of an ectopic beat, the scan is repeated at the same position. With this approach, the application spectrum of the prospective sequential technique can be extended to patients with high and irregular heart rates, with typical doses in the range of 1–3 mSv [23] (Table 2).

An additional technique to acquire cardiac CT data is the prospectively ECG-triggered dual-source high-pitch mode which requires the use of a dual-source CT system [24]. In this approach, a high-pitch of 3.4 is used with a table moving at a speed of 450 mm/s (Somatom Definition Flash) or 737 mm/s (Somatom Force). The patient's ECG is used to trigger the start of table motion such that after acceleration to maximum table speed a pre-selected z-position (e.g., the base or the apex of the heart) is reached at a pre-selected cardiac phase. With this scan technique, the entire cardiac volume is acquired in a single heartbeat, with a scan time $<0.3$ s at 450 mm/s and $<0.2$ s at 737 mm/s. Note that the temporal resolution of the individual images is 75 ms resp. 66 ms. Because no data redundancies are needed in this type of acquisition, it is possible to further reduce radiation dose compared to the conventional prospective technique [25]. This technique however is recommended for patients with heart rates below 65 bpm (Somatom Definition Flash) and below 75 bpm (Somatom Force). Using these two scanners routine doses of approximately 1 [26] and 0.6 mSv [27] can be achieved, respectively.

## Radiation Exposure Adaptation by Selecting the X-ray Tube Potential

The polychromatic spectrum of X-ray photons delivered to the patient is controlled by the selection of different tube potentials at which an X-ray tube can operate. The tube potential selection has three main consequences: (1) the kV influences radiation exposure, (2) since the kV has an impact on overall radiation exposure it likewise has an effect on image noise, (3) the kV directly impacts image contrast of radiological relevant materials (and tissues) such as calcium and iodine. Traditionally, 120 kV was the most common tube potential for scanning adult patients that provided a reasonable mix of X-ray penetration and image contrast. Using kV values below 120 was challenging due to the limits of X-ray tubes that could not deliver enough power at low kV values. However, in many situations, a setting of 120 kV may not be the best choice for a given patient or type of exam. For that reason, there is a recent trend to scan patients at various kV values depending on patient size [28] and type of examination.

Image quality of CT images, at a given spatial resolution and slice thickness, is mainly characterized by two parameters: contrast and noise. Improving one or both of these parameters will result in improved image quality, hence, potentially helping the reading physician to make a more precise diagnosis. For example, if the contrast increases but the noise remains unchanged, the image quality improves. Often, iodinated contrast agents are

**Table 2** Typical effective dose values for various coronary CT angiography techniques using dual-source CT

| Coronary CTA technique | Effective dose (mSv) | References |
|---|---|---|
| Retrospective (spiral) | 4.0–14.0 | [21, 22, 77] |
| Prospective (sequential) | 1.0–3.0 | [23, 78] |
| Prospective flash mode (spiral) | 1.0 | [26, 79] |
| Prospective turbo flash mode (spiral) | 0.6 | [27] |

administered to improve contrast and the visibility of the organ structures in CT images. In these cases, image contrast increases as the X-ray tube voltage is reduced since low energy X-rays are more strongly absorbed by iodine than by the surrounding tissue. Usually as a result of lowering kV, the tube current must be increased in order to maintain similar noise levels.

Tissue contrast and image noise are often combined into the single term of contrast-to-noise ratio (CNR) the ratio of the difference between the tissue of interest (TOI) and the background (BG) divided by the standard deviation of the BG:

$$\mathrm{CNR} = \frac{\mathrm{Contrast}}{\mathrm{Noise}} = \frac{\mathrm{Mean\ HU\ (TOI)} - \mathrm{Mean\ \ HU\ (BG)}}{\mathrm{Stdev\ \ HU\ (BG)}}.$$

For a constant CNR in CT angiography studies (or others utilizing contrast material), the radiation dose can be significantly reduced by choosing lower X-ray tube voltages than 120 kV. For larger or obese patients that have higher X-ray attenuation, the output current of the X-ray tube at lower kV settings or even 120 kV may not be sufficient to produce desired CNRs. Limited tube flux or photon penetration will reduce the number of photons that reach the detector and contribute to the image reconstruction causing photon starvation artifacts such as streaks or cupping. For these patients, scanning at higher X-ray tube voltages such as 140 kV may be necessary to achieve a better CNR at similar dose (vs. 120 kV) due to improved image noise, despite the resulting reduction in iodine contrast. In the case of a neonatal or pediatric patient scanned at 120 kV, either lowering the number of photons delivered by reducing the mAs or lowering the kV, should be considered as either way provides great potential for dose reduction.

Previous investigations have advocated for the use of lower kV values and provided strategies for the manual selection of kV according to patient size and examination type [28–31]. As aforementioned, reductions in the kV need to be accompanied by adjustment in the tube current to balance the contrast improvement and control the noise increase. Consequently, the interrelationship among kV, mAs, dose, contrast, and noise for determining the optimal scan settings for an individual patient is complex, time-consuming, and very challenging to implement in a busy clinical environment Therefore, it is not surprising that kV is rarely optimized for an individual patient and exam type in routine clinical practice. However, tools such as CARE kV™ (Siemens Healthcare) have been developed to automatically recommend the optimal kV setting for each individual patient and specific exam type allowing one to tap into this significant unused potential for dose reduction. CARE kV utilizes the patient attenuation information gathered by the CT localizer radiograph (i.e., topogram) along with user provided 'diagnostic task' selections by manipulating a slider bar (Fig. 4), to optimize kV and mAs such that the user-chosen CNR ratio is maintained. As a result, the desired image quality can be achieved at the lowest possible dose.

With CARE Dose4D, the main goal is to maintain a consistent image quality by controlling image noise. With CARE kV, the key image quality parameter to control is the CNR ratio. The system calculates the patient-specific mAs curves for all possible kVp levels based on the scan range, anatomical region, and type of exam (also called "tissue of interest") necessary to deliver the desired image quality. Based on these curves, the system finds the optimal setting for dose efficiency and then checks whether this optimal setting is possible (due to tube current limits, pitch settings, scan range, etc.). If it is not possible, the next best kV setting is selected.

To explain the benefit of CARE kV, we can use the example of a checkerboard-like pattern (Fig. 5a). In this case, the difference between light and dark squares would be our contrast and the standard deviation (for simplicity, equal in both squares) would be the noise. If we assume (for simplicity) that the image in Fig. 5a has a CNR equal to 1, then doubling the amount of noise would result in the image with a CNR of 0.5 (Fig. 5b). In this case, the ability to see the boundaries between light and dark squares would

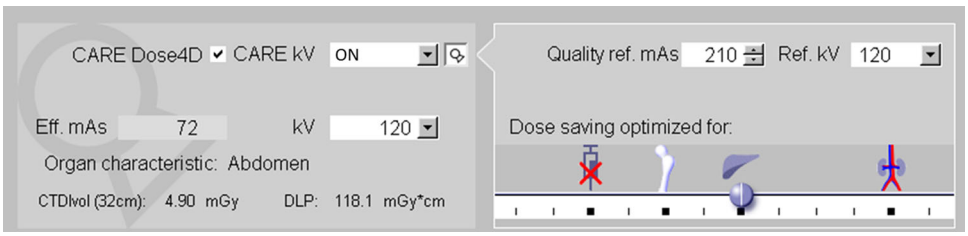


**Fig. 4** The CARE kV user interface. With the CARE kV tool turned "*On*," the Quality Reference mAs and Reference kV of the specific exam are used to determine and maintain image quality in conjunction with the CARE kV slider, which is used to indicate the type of exam being performed (non-contrast, contrast-enhanced, angiography). The automatically calculated optimal kV and mAs settings are shown on the *left*

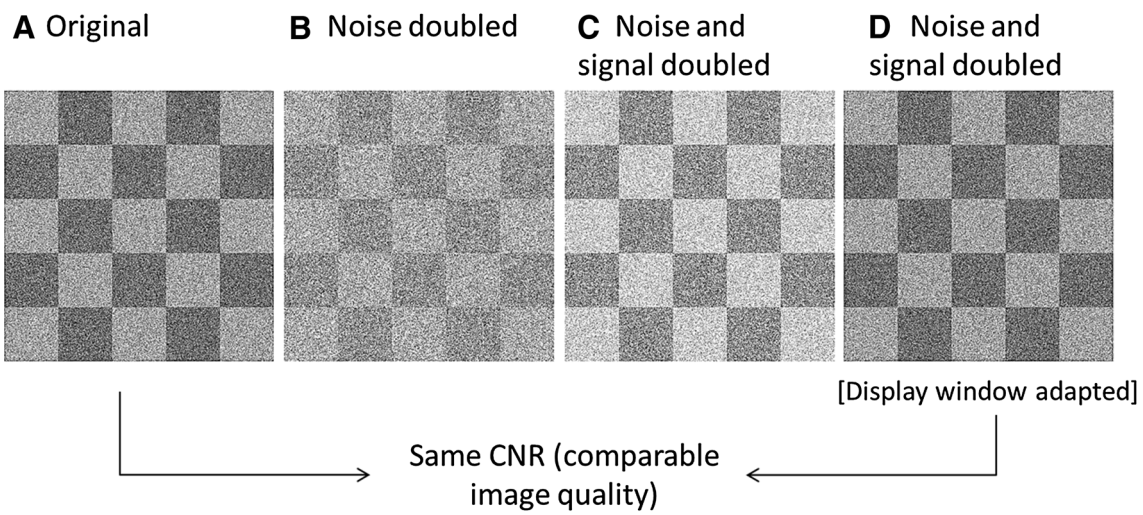


**Fig. 5** Impact of image noise and signal changes in contrast-to-noise ratio (CNR). When the signal and noise from the original image are doubled the CNR is maintained (**c**); however, a display window adaptation (**d**) is needed to more clearly notice the maintenance of CNR relative to the original image (**a**)

become more difficult even though the same amount of contrast exists in the image. If, in addition to the doubling of image noise, we would also double the difference between the TOI and BG, the resulting image would then regain a CNR of 1 (Fig. 5c). In this case, the ability to perceive the light and dark squares would also be regained, but the overall image would have a different appearance to the reader. If we would also adjust the display window to take into account the higher contrast and noise, we could generate an image that looks exactly the same as the original image in spite of having twice the amount of noise and twice the amount of contrast (Fig. 5d).

Maintaining the same noise level at lower kV values requires a significant increase in mAs. However, for high contrast examinations such as CT angiography, effective mAs can be reduced relative to the constant noise level resulting in a decreased dose while maintaining CNR. For example, the CT values of iodine-enhanced vessels at 80 kV are approximately two times higher than at 140 kV. Hence, the noise level can be twice as high while still maintaining the original CNR and permitting an exam at a significantly reduced dose. In non-contrast exams, there is little or no additional benefit gained from contrast improvement at lower kV. However, the CARE kV tool will still work to optimize the scan settings to the individual patient.

Substantial dose reductions have been demonstrated with CARE kV ranging from 20 to 70 %, relative to scanning with 120 kV. It is important to note that these dose reductions were achieved while maintaining or even improving image quality in CT applications such as CT angiography [32], contrast-enhanced body imaging applications [33], cardiac CT [3] and pediatric CT examinations [34•, 35, 36].

## Iterative Reconstruction

The traditional method of image reconstruction in CT is the so-called filtered back-projection (FBP). A distinctive aspect of the FBP is that the user can choose different kernels (filters) that allow to trade-off between spatial resolution and image noise. For example, softer kernels are typically used for visualization of soft tissues because they lead to lower noise but come at the cost of a lower spatial resolution. On the contrary, sharper kernels that are often used for visualization of the lungs or bones lead to a better spatial resolution but have a considerably higher image noise. Another distinctive aspect of the FBP is that it does not incorporate any statistical model or modeling of the CT system. As a result, all CT projections are treated the same, independent of their quality, and the artifacts caused by specific features of the CT system geometry (e.g., cone-beam) cannot be corrected for during the reconstruction.

Statistical IR (also known as 'theoretical' or 'model-based') is an approach to image reconstruction in which modeling of the statistical properties of the X-ray projection data can be incorporated [37]. Additionally, modeling of the CT system optics can be used to improve spatial resolution. Furthermore, since IR is not a linear method, the fundamental limitation of FBP (tradeoff of noise and spatial resolution) does not necessarily apply, As a result, image noise can potentially be improved without a loss of spatial resolution.

A general framework for statistical IR incorporates a model to handle data statistics, a regularization function in the image space, and a forward projection loop that requires a model of the CT system acquisition (Fig. 6) [38].

Independent of the specific implementation, the two main benefits of IR are manifested in noise reduction and

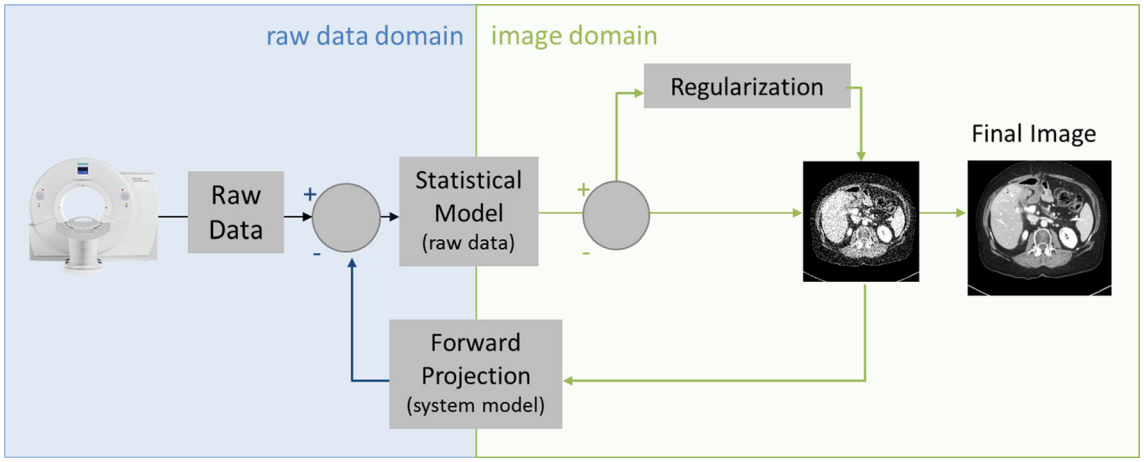


**Fig. 6** Diagram illustrating a generalized approach to statistical iterative reconstruction, also called model-based iterative reconstruction

reduction of image artifacts. The regularization mechanism, applied in the image domain, ensures convergence of the IR process and strongly affects noise reduction and, to a lesser extent, the statistical modeling step in the raw data domain. On the other hand, the statistical modeling in the raw data domain and, more importantly, the forward projection loop are mostly responsible for artifact reduction. The statistical modeling helps reduce photon starvation streaks in the areas of very high attenuation (e.g., shoulders), while the forward projection loop helps reduce artifacts caused by the non-exact nature (in mathematical sense) of the FBP algorithm. However, the forward projection loop is the most computationally expensive step compared to the regularization and statistical modeling.

Various generations of IR from different CT manufacturers can be distinguished in terms of how they address the trade-off between the computational efficiency and the benefits of noise and artifact reduction (Table 3). For example, Siemens initially offered the Iterative Reconstruction in Image Space (IRIS$^{TM}$, Siemens Healthcare) that primarily focused in the noise reduction aspect of IR (the regularization step). This method has been shown to reduce image noise on acquisitions with 30–50 % reduced dose in applications such as abdominal CT [39], CT enterography [40], and cardiac CT [41]. The Sinogram Affirmed Iterative Reconstruction (SAFIRE$^{TM}$, Siemens Healthcare) introduced the forward projection loop and statistical modeling in the image domain with the purpose to reduce artifacts (e.g., cone-beam and high-pitch spiral), further enhance noise reduction [42, 43•, 44] and improve spatial resolution [45–47]. The most recently introduced Advanced Modeled Iterative Reconstruction (ADMIRE$^{TM}$, Siemens Healthcare) uses an advanced statistical modeling both in the projection and image domains. Instead of a basic regularization function that promotes smoothness [37], ADMIRE uses a function that separates actual signal information from noise, and operates in a larger voxel neighborhood (in both the in-plane and longitudinal directions) which is not restricted locally (i.e., immediate voxel neighbors) [48•]. As a result, it is possible not only to even further reduce image noise but also better preserve the natural appearance (texture) of CT images [49]. The degradation of image texture, that is, making the CT image appearance overly smooth ('plastic' looking) has been reported as a major limitation of IR methods, particularly when the strongest noise reduction level was used [50]. Finally, advanced statistical modeling in the raw data domain in conjunction with a pre-conditioning filter (i.e., weighted filtered back projection) allows to accelerate the convergence of the ADMIRE algorithm [51]. This translates into a more efficient computation, in spite of the added mathematical complexity. As a result, the ADMIRE reconstruction times are only a few times longer than the reconstruction times with conventional FBP, making it fully acceptable in a busy clinical environment.

**Table 3** Commercially available iterative reconstruction algorithms by various CT manufacturers

| Vendor | Product Name |
|---|---|
| General Electric | ASIR, VEO |
| Hitachi | Intelli IP |
| Neusoft | AIR |
| Philips | iDOSE, IMR |
| Siemens | IRIS, SAFIRE, ADMIRE |
| Toshiba | AIDR 3D |

There are two major uses for IR algorithms:

1. Image noise reduction for acquisitions with reduced radiation dose (e.g., decreased tube current and/or the tube potential).

2. Improvement of the image quality by reducing noise, suppressing image artifacts, and improving spatial resolution.

It is important to clarify that IR does not always reduce radiation dose automatically. To reduce the dose, the user has to set up a new CT protocol that employs a lower dose compared to the standard dose protocol. For example, in addition to standard (FBP) protocols, Siemens users can select alternative (IR) protocols in which the quality reference mAs (hence, dose) is reduced (e.g., by 30 %) and images are reconstructed using IR methods such as IRIS or SAFIRE. With the introduction of the latest generation dual-source CT system, the Somatom Force, all default protocols operate at a lower dose and employ ADMIRE.

## Advanced CT Acquisition Modes in Last Generation CT Scanners

### Dual-Energy CT

Dual-energy CT refers to scanning using two kilovoltage values simultaneously: low and a high kV values. The DECT data can be used to generate images which are equivalent to conventional single-energy CT (e.g., routine 120 kV images). In addition, it is possible to generate material-specific images through dual-energy postprocessing. A primary example of material-specific imaging is the identification and quantification of iodine, which can then be selectively removed from contrast-enhanced images; hence, generating 'virtual' non-contrast images [52]. It has been shown that the use of virtual non-contrast imaging (sometimes also called virtual unenhanced imaging) can potentially reduce the radiation dose by up to 50 % in two-phase CT examinations, with the true-non-contrast CT acquisition replaced with the virtual non-contrast images [53].

In recent years, several manufactures have introduced CT scanners that allow this type of data acquisition including dual-source CT [54], single-source fast kV switching (also known as Gemstone Spectral Imaging or GSI) [55], and the two-layered detectors [56]. The two most common kVs for dual-energy CT are 80 and 140 kV. However, state-of-the-art dual-source CT systems offer a wider range of possibilities for the kV pairs and typically employ additional filtration of the high-kV tube to increase the spectra separation [57•]: 80/Sn140 kV and 100/Sn 140 kV (Somatom Definition Flash); and 70/Sn150 kV, 80/Sn150 kV, 90/Sn150 kV and 100/Sn150 kV (Somatom Force), where Sn denotes the additional tin filter. The tin filter removes the lower energy portions of the high-kV spectrum and shifts its mean energy to higher values, in this way increasing spectral separation. The flexibility of the dual-source system in dual-energy kV pairs allows the pairing to be tailored to the patient size, and exams type by independently controlling the tube current applied to each X-ray tube as well. This is very important because dose reduction features such as AEC or organ-dose modulation ("Automated exposure control of the tube current" section) can be simultaneously used with this type of acquisition, which is not possible in most single-source approaches to date. Further, dual-source dual-energy CT is also compatible with IR methods such as SAFIRE or ADMIRE ("Iterative reconstruction" section). Hence, similar strategies for an optimization of radiation dose and image quality can be pursued with dual-energy CT just as with conventional (single-energy) CT. Various investigators have shown that the radiation doses (and corresponding image quality) of dual-energy CT are similar or better to conventional (single-energy) CT [58, 59].

### Selective Photon Shielding in Conventional CT for Ultra-Low Dose Non-Contrast Imaging

One of the very latest advances in CT is the introduction of additional filtration ("selective photon shield") in front of the X-ray tube. Such filtration results in attenuation of the lower energy photons and hardening the X-ray spectrum (Fig. 7). Similar photon shields were used before in dual-energy CT with the purpose to increase the spectra separation [60]. However, in this case, the purpose of the selective photon shield is to improve the dose efficiency (i.e., achieve less noise at the same radiation dose) of conventional single-energy CT for specific types of exams (e.g., differentiating soft tissue and air in low-dose lung

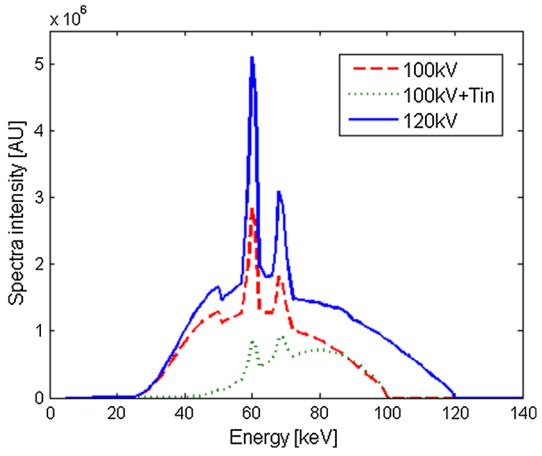


**Fig. 7** Comparison of three polychromatic X-ray spectra used in CT. 100 kV, 100 kV with added spectra filtration with Tin (100 kV + Tin), and 120 kV; with corresponding mean energies of 59, 72, and 64 keV, respectively. The selective photon shield made of tin attenuates the lower energy photons, hence increasing the mean photon energy of the spectra

cancer screening). Because the selective photon shield hardens the X-ray beam, it is not intended for use in contrast-enhanced examinations due to reduced iodine signal. This technology has become available on the Somatom Force (Siemens Healthcare, Forchheim, Germany). The photon shield is made of tin and can be mechanically placed in front of the X-ray tube when the user selects this scan protocol. The selective photon shield is available when the X-ray tube operates at either 100 (Sn100) or 150 kV (Sn150). The first reported application of this technology, in conjunction with ADMIRE, was ultra-low dose non-enhanced chest CT imaging with Sn100 kVp [48•]. The investigators found that high sensitivity for pulmonary nodules detection was still possible with dose as low as 0.06 mSv. Using a similar type of acquisition and reconstruction, Newell et al. demonstrated in a phantom study that it was possible to obtain accurate attenuation values in a broad range of material densities and maintain acceptable image noise levels, while using radiation output levels as low as 0.15 mGy [61]. According to the authors, the resulting radiation doses are comparable with that of 2-view digital projection chest radiography. An example application of this technology is shown in Fig. 8. Other applications of the selective photon shield are expected in areas such as low-dose CT colonography and other non-contrast CT applications which typically use lower doses than routine CT examinations.

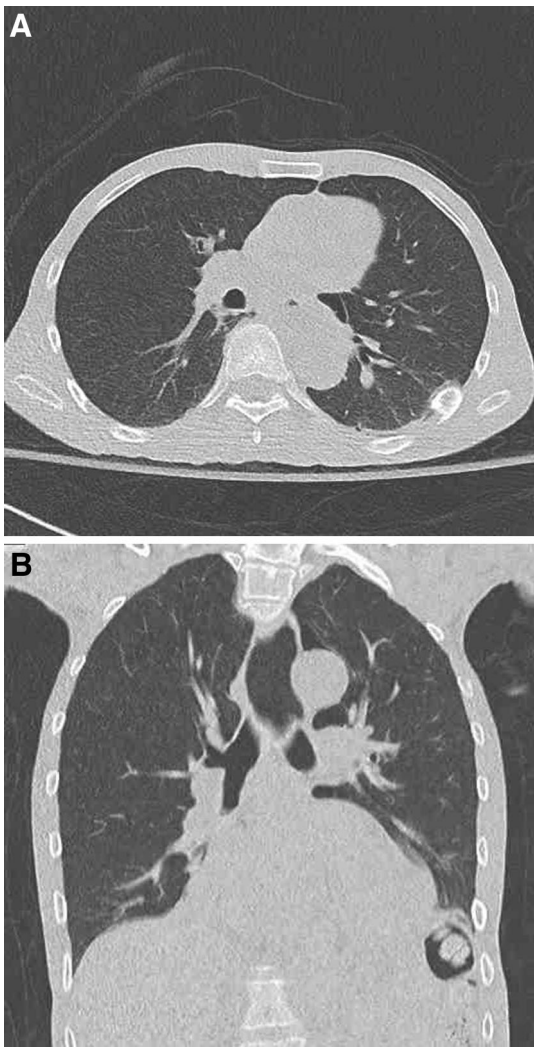


**Fig. 8** Lung CT scan using 100 kV with added spectra photon shield made of Tin. **a** Axial and **b** coronal view. The CT study was acquired with $CTDI_{vol} = 0.37$ mGy and DLP = 12.8 mGy cm. Estimated effective dose was 0.17 mSv. Image was reconstructed using advanced modeled iterative reconstruction (ADMIRE). Copyright 2014 Mayo Foundation for Medical Education and Research

## Advances in CT Scanner Hardware Components

The improvements in each of the hardware components of a CT imaging system have substantial influence on its radiation dose reduction capabilities. Two of the essential components in every CT system are the X-ray tube and the CT detectors (Fig. 9).

The X-ray tube is typically characterized by the range of tube potential values at which it can operate (typically 80–140 kV), the maximum tube current (typically 400–800 mA), and the tube power (typically 50–100 kW). Expanding the range of possible tube potential values can help to individualize CT scans to patients and type of examinations. For example, the Straton® X-ray tube (Siemens Healthcare) operates with a tube potential as low as 70 kV. Operation at such a low kV has been found to be particularly useful for contrast-enhanced and CT angiography applications in pediatric patients [34•] and for scanning the neck [62]. The use of 70 kV however has not been common in routine adult applications, primarily because of the limiting power available with this low kV.

The recently introduced Vectron® X-ray tube (Siemens Healthcare) has the ability to substantially increase the tube current even at low kV values. Specifically, the tube current can be increased up to 1,300 mA at 70 kV, hence, enabling the use of this reduced kVp even for adult patients (Fig. 10). Furthermore, the Vectron tube offers greater flexibility to tube potential selection between 70 and 150 kV (in steps of 10 kV), and hence adds the possibility to further customize the CT examination [63•]. With the wider range of available kV values, it becomes more important to use technologies such as CARE kV that can automatically select the optimal combination of kV and mAs for each patient size and diagnostic application in order to achieve the desired image quality at the lowest dose. The tube power reserve can be doubled with the dual-source CT technology, when two X-ray tubes are simultaneously operated at the same tube potential. Specifically,

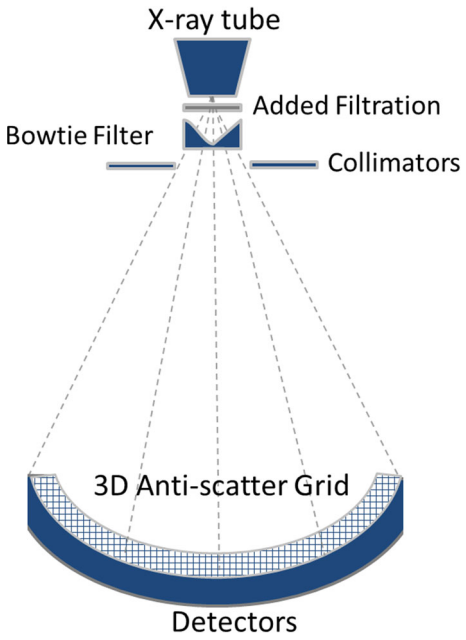


**Fig. 9** Schematics illustrating essential CT hardware components in a modern CT scanner

this means that it is possible to reach up to 2 × 120 kW for the latest generation dual-source CT (Somatom Force). The increase in power reserve enables a sufficient photon flux for fast acquisition modes such as high-pitch CT scanning or cardiac imaging, hence obviating the need to sacrifice image quality for the acquisition speed.

Besides the X-ray sources, several other hardware components can also have an important impact on radiation dose reduction. For example, the use of adaptive collimators can reduce the over-scanning in spiral CT scans [64] and the use of dedicated bowtie filters can reduce the dose for cardiac or pediatric applications [54].

On the CT detectors end, some of the latest advances include the reduction of electronic noise, improved spatial resolution, larger detector coverage, and improved scatter correction with anti-scatter grids. The latest generation of CT detectors introduced (e.g., the Stellar® and Stellar$^{Infinity}$ detectors, Siemens Healthcare) combines the electronics of the photodiode and the analog-to-digital converter into a single-integrated circuit, hence, obviating the need for analog connections. This design has a major impact on the reduction of electronic noise. At routine radiation dose levels, image noise is primarily driven by quantum with electronic noise playing a secondary role. However, when the photon flux reaching the detector is very low the electronic noise can not only dramatically increase the image noise but also cause streaking artifacts (known as "photon starvation"). Thus, the use of improved electronics for CT detectors, that minimizes electronic noise, can improve the image quality and dose efficiency in

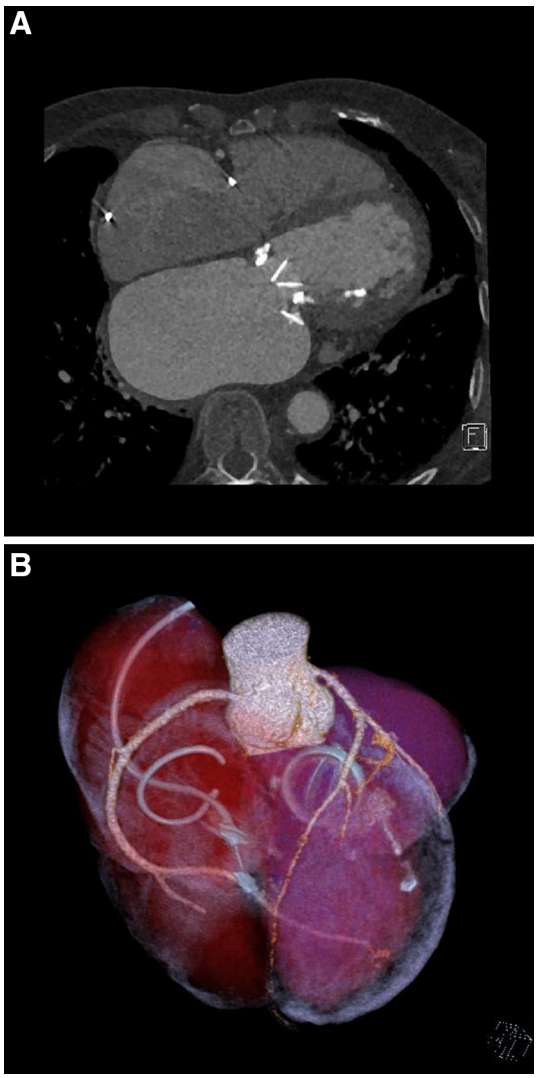


**Fig. 10** CT scan of an aortic valve in an adult patient with a heart rate of 50 bpm. **a** Reformatted image view and **b** three-dimensional reconstruction. The CT scan was acquired using a fast acquisition technique with high-pitch dual-source CT technique (TurboFlash$^{TM}$) which only needed 0.22 s to cover 157 mm at a pitch of 3.2. Acquisition settings were 70 kV and 540 effective mAs. The resulting dose values were $CTDI_{vol}$ = 1.52 mGy and DLP = 30 mGy cm, with estimated effective dose of 0.42 mSv. Courtesy of University Hospital Zurich, Switzerland

applications such as scanning morbidly obese patients [65, 66], reduced dose chest CT for lung cancer screening [48•], reduced dose CT scans for urolithiasis [67], or CT colonography [68, 69]. Furthermore, the synergistic use of IR with the Stellar detector technology also allows to decrease detector-to-detector crosstalk resulting in improved spatial resolution. This effect has been demonstrated for applications such as cardiac CT with improved depiction of coronary stents [70, 71]. Besides, the use of detectors with reduced electronics noise, in conjunction with additional high-resolution combs which are mechanically placed in

front of the detectors, allow further improvements in spatial resolution that have been demonstrated for applications such as temporal bone imaging [72, 73].

The availability of systems with wider detectors (cone-beam >4 cm) in conjunction with a high rotation speed enables a faster CT acquisition in combination with dual-source CT technology [74] or very wide CT detectors with geometries of up to 320-detector rows [75]. However, wider cone-beam systems are more prone to scatter radiation which may impact low-contrast CT applications. To compensate for this potential negative effect in image quality, various CT manufacturers have introduced more advanced anti-scatter grids, instead of traditional one-dimensional anti-scatter grids [76]. For example, the detector module of the Somatom Force, which covers approximately 6 cm in the z-axis, is coupled with an advanced anti-scatter grid that blocks scattered photons more efficiently and, hence, substantially improves the low-contrast detectability, especially in combination with IR (ADMIRE). This effect has been demonstrated in a recent study in an adult population undergoing abdominal portal-venous CT examinations [49].

## Conclusion

The new CT technologies such as the automated selection of the tube current and the tube potential as well as IR are powerful tools for optimization of CT protocols. A combination of these three technologies can help substantially reduce radiation dose while maintaining image quality. More importantly, this combined approach offers an opportunity to tailor the CT exam to each individual patient and to each specific diagnostic task. These technologies are further enhanced by the continuous progress in CT hardware: X-ray tubes, CT detectors, and other components. The novel approaches such as dual-energy CT and ultra-low dose scanning with the selective photon shield present new exciting opportunities for radiation dose reduction with maintained image quality. Finally, it is very important to highlight the vital role that radiologists, CT technologists, and medical physicists have in this arena; it is essential that they are familiar with the development of new technologies available in CT scanners such that these can be effectively used to improve care for patients by providing individualized CT examinations that consistently use low radiation dose while achieving reliable diagnostic image quality.

### Compliance with Ethics Guidelines

**Conflict of Interest** Dr. Juan C. Ramirez-Giraldo is a full time employee of Siemens Medical Solutions USA, Inc. Dr. Matthew Fuld is an employee of Siemens Medical Solutions USA, Inc. Dr. Katharine Grant is a full time employee of Siemens Medical Solutions USA, Inc. Dr. Andrew N. Primak is a full time employee of Siemens Medical Solutions USA, Inc. Dr. Thomas Flohr is an employee of Siemens Healthcare, Forchheim, Germany.

**Human and Animal Rights and Informed Consent** This article does not contain any studies with human or animal subjects performed by any of the authors.

## References

Papers of particular interest, published recently, have been highlighted as:

- Of importance


1. Wilting JE, Zwartkruis A, Leeuwen MS, Timmer J, Kamphuis AG, Feldberg M. A rational approach to dose reduction in CT: individualized scan protocols. Eur Radiol. 2001;11:2627–32.
2. Frush DP, Soden B, Frush KS, Lowry C. Improved pediatric multidetector body CT using a size-based color-coded format. Am J Roentgenol AJR. 2002;178:721–6.
3. Layritz C, Muschiol G, Flohr T, Bietau C, Marwan M, Schuhbaeck A, Schmid J, Ropers D, Achenbach S, Pflederer T. Potential for radiation dose savings in abdominal and chest CT using automatic tube voltage selection in combination with automatic tube current modulation. J Cardiovasc Comput Tomogr. 2013;7(5):303–10.
4. McCollough CH, Zink FE, Kofler J, Matsumoto JS, Thomas KB, Hoffman AD. Dose optimization in CT: creation, implementation and clinical acceptance of size-based technique charts. Radiology. 2002;225:591.
5. Goske M, Applegate K, Bulas D, Buttler P, Callahan M. Image gently five years later: what goals remain to be accomplished in radiation protection for children? Am J Roentgenol AJR. 2012;199(3):477–9.
6. Image wisely: radiation safety in adult medical imaging. American College of Radiology and Radiological Society of North America. http://www.imagewisely.org. Accessed 30 Oct 2014.
7. ESR. EUROSAFE Imaging. European Society of Radiology. http://www.eurosafeimaging.org/. Accessed 30 Oct 2014.
8. Kalra MK, Mahe MM, Toth TL, Schmidt B, Westerman BL, Morgan HT, Saini S. Techniques and applications of automatic tube current modulation for CT. Radiology. 2004;233(3):649–57.
9. Soderberg M, Gunnarsson M. Automatic exposure control in computed tomography—an evaluation of systems from different manufacturers. Acta Radiol. 2010;51(6):625–34.
10. Zacharia TT, Kanekar SG, Nguyen DT, Moser K. Optimization of patient dose and image quality with z-axis dose modulation for computed tomography (CT) head in acute head trauma and stroke. Emerg Radiol. 2010;18(2):103–37.
11. Frush DP. Overview of CT technologies for children. Pediatr Radiol. 2014;44(3):S422–6.
12. Papadakis A, Perisinakis K, Damilakis J. Automatic exposure control in pediatric and adult multidetector CT examinations: a phantom study on dose reduction and image quality. Med Phys. 2008;35(10):4567–76.
13. NEMA. NEMA XR 29-2013: standard attributes on CT equipment related. Rosslyn: National Electrical Manufacturers Association; 2013.
14. AAPM. CT scan parameters: translation of terms for different manufacturers. American Association of Physicists in Medicine AAPM, 20 April 2012. https://www.aapm.org/pubs/CTProtocols/. Accessed 02 Sep 2014.

15. Duan X, Wang J, Christner JA, Leng S, Grant KL, McCollough CH. Dose reduction to anterior surfaces with organ-based tube current modulation: evaluation of performance in a phantom study. Am J Roentgenol AJR. 2011;197:689–95.
16. Vollmar SV, Kalender WA. Reduction of dose to female breast in thoracic CT: a comparison of stardard-protocol, bismuth-shielded, partial and tube-current-modulated CT examinations. Eur Radiol. 2008;18:1674–82.
17. Lungren MP, Yoshizumi TT, Brady SM, Toncheva G, Anderson-Evans C, Lowry C, Zhou XR, Frush D, Hurwitz LM. Radiation dose estimations to the thorax using organ-based dose modulation. Am J Roentgenol AJR. 2012;199(1):W65–73.
18. Wang J, Duan X, Christner JA, Leng S, Grant KL, McCollough CH. Bismuth shielding, organ-based tube current modulation, and global reduction of tube current for dose reduction to the eye at head CT. Radiology. 2012;262(1):191–8.
19. Wang J, Duan X, Christner JA, Leng S, Yu L, McCollough CH. Radiation dose reduction to the breast in thoracic CT: comparison of bismuth shielding, organ-based tube current modulation, and use of a globally decreased tube current. Med Phys. 2011;38(11):6084–92.
20. McCollough CH, Wang J, Gould RG, Orton CG. Point/counterpoint. The use of bismuth breast shields for CT should be discouraged. Med Phys. 2012;39(5):2321–4.
21. Jakobs TF, Becker CR, Ohnesorge B, Flohr T, Suess C, Schoepf UJ, Reiser MF. Multislice helical CT of the heart with retrospective ECG gating: reduction of radiation exposure by ECG-controlled tube current modulation. Eur Radiol. 2002;12(5):1081–6.
22. Stolzmann P, Scheffel H, Schertler T, Frauenfelder T, Leschka S, Husmann L, Flohr T, Marincek B, Kaufmann P, Alkadhi H. Radiation dose estimates in dual-source computed tomography coronary angiography. Eur Radiol. 2008;18(3):592–9.
23. Stolzmann P, Leschka S, Scheffel H, Krauss T, Desbiolles L, Plass A, Genoni M, Flohr TG, Wildermuth S, Marincek B, Alkadhi H. Dual-source CT in step-and-shoot mode: noninvasive coronary angiography with low radiation dose. Radiology. 2008;249(1):71–80.
24. Achenbach S, Marwan M, Schepis T, Pflederer T, Bruder H, Allmendiger T, Petersilka M, Anders K, Lell M, Kuettner A, Ropers D, Daniel W, Flohr T. High-pitch spiral acquisition: a new scan mode for coronary CT angiography. J Cardiovasc Comput Tomogr. 2009;3(2):117–21.
25. Flohr TG, Leng S, Yu L, Allmendinger T, Bruder H, Petersilka M, Eusemann CD, Stierstorfer K, Schmidt B, McCollough CH. Dual-source spiral CT with pitch up to 3.2 and 75 ms temporal resolution: image reconstruction and assessment of image quality. Med Phys. 2009;36(12):5641–53.
26. Lell M, Marwan M, Schepis T, Pflederer T, Anders K, Flohr T, Allmendinger T, Kalender W, Ertel D, Thierfelder C, Kuettner A, Ropers D, Daniel WG, Achenbach S. Prospectively ECG-triggered high-pitch spiral acquisition for coronary CT angiography using dual source CT: technique and initial experience. Eur Radiol. 2009;19(11):2576–83.
27. Morsbach F, Gordic S, Desbiolles L, Husarik D, Frauenfelder T, Schmidt B, Allmendinger T, Wildermuth S, Alkadhi H, Leschka S. Performance of turbo high-pitch dual-source CT for coronary CT angiography: first ex vivo and patient experience. Eur Radiol. 2014;24(8):1889–95.
28. Siegel M, Schmidt B, Bradley D, Suess C, Hildebolt C. Radiation dose and image quality in pediatric CT: effects of technical factors and phantom size and shape. Radiology. 2004;233(2):515–22.
29. Kalender WA, Deak P, Kellermeier M, Van Straten M, Vollmar SV. Application- and patient size-dependent optimization of x-ray spectra for CT. Med Phys. 2009;36(3):993–1007.
30. Arch ME, Frush DP. Pediatric body MDCT: a 5-year follow-up survey of scanning parameters used by pediatric radiologists. Am J Roentgenol AJR. 2008;191:611–7.
31. Kim J-E, Newman B. Evaluation of a radiation dose reduction strategy for pediatric chest CT. Am J Roentgenol AJR. 2010;194:1188–93.
32. Goetti R, Winklehner A, Gordic S, Baumueller S, Karlo CA, Frauenfelder T, Alkadhi H. Automated attenuation-based kilovoltage selection: preliminary observations in patients after endovascular aneurysm repair of the abdominal aorta. Am J Roentgenol AJR. 2012;199(3):W380–5.
33. Mayer C, Meyer M, Fink C, Schmidt B, Sedlmair M, Schoenberg SO, Henzler T. Potential for radiation dose savings in abdominal and chest CT using automatic tube voltage selection in combination with automatic tube current modulation. Am J Roentgenol AJR. 2014;203(2):292–9.
34. • Siegel MJ, Hildebolt C, Bradley D. Effects of automated kilovoltage selection technology on contrast-enhanced pediatric CT and CT angiography. Radiology. 2013;268(2):538–47. *This was one of the earliest studies reporting the benefits in dose reduction using automated tube potential selection in pediatric CT of the body. Relative to CT scans with 120 kVp, the average estimated dose reductions were 27%, and as much as 49% for CT angiography.*
35. Siegel MJ, Ramirez-Giraldo JC, Hildebolt C, Bradley D, Schmidt B. Automated low-kilovoltage selection in pediatric computed tomography angiography: phantom study evaluating effects on radiation dose and image quality. Invest Radiol. 2013;48(8):584–9.
36. Brinkely M, Ramirez-Giraldo J, Samei E, Frush D. Effects of automatic tube potential selection on radiation dose, image quality and lesion detectability in pediatric abdominopelvic CT and CTA: a phantom study. Pediatr Radiol. 2014;44:S88.
37. Thibault J-B, Sauer KD, Bouman CA, Hsieh J. A three-dimensional approach to improved image quality for multislice helical CT. Med Phys. 2007;34(11):4526–44.
38. Nuyts J, DeMan B, Fessler JA, Zbijewski W, Beekman FJ. Modelling the physics in the iterative reconstruction for transmission computed tomography. Phys Med Biol. 2013;58:R63–96.
39. Schindera ST, Diedrichsen L, Muller HC, Rusch O, Marin D, Schmidt B, Raupach R, Vock P, Szucs-Farkas Z. Multidetector CT at different tube voltages: assestment of diagnostic accuracy, image quality, and radiation dose in a phantom study. Radiology. 2011;260(2):454–62.
40. Lee S, Park S, Kim A, Yang S, Yun S, Lee S, Jung G, Ha H. A prospective comparison of standard-dose CT enterography and 50% reduced-dose CT enterography with and without noise reduction for evaluating Crohn disease. Am J Roentgenol AJR. 2011;197(1):50–7.
41. Park E, Lee W, Kim KW, Thomas A, Chung J, Park J. Iterative reconstruction of dual-source coronary CT angiography: assessment of image quality and radiation dose. Int J Cardiovasc Imaging. 2012;28(7):1775–86.
42. Remer E, Herts B, Primak A, Obuchowski N, Greiwe A, Roesel D, Purysko A, Feldman M, De S, Shah S, Dong F, Monga M, Baker M. Detection of urolithiasis: comparison of 100% tube exposure images reconstructed with filtered backprojection and 50% tube exposure images reconstructed with sinogram-affirmed iterative reconstruction. Radiology. 2014;272(3):749–56.
43. • Goenka A, Herts B, Obuchowski N, Primak A, Dong F, Karim W, Baker M. Effect of reduced radiation exposure and iterative reconstruction on detection of low-contrast low-attenuation lesions in an anthropomorphic liver phantom: an 18-reader study. Radiology. 2014;272(1):154–63. *This rigorous study enrolled 18 readers and found that for the challenging task of low-contrast low-attenuation liver lesions, dose reduction with iterative*

*reconstruction were more modest than typically reported in other studies. Dose reductions found with this study ranged from 25–50%. The study found that a major benefit with iterative reconstruction was higher confidence in readers but not necessarily better detectability.*

44. Schindler A, Vliegenthart R, Schoepf U, Blanke P, Ebersberger U, Cho Y, Allmendiger T, Vogt S, Raupach R, Fink C, Saam T, Bamberg F, Nikolau K, Apfaltrer P. Iterative image reconstruction techniques for CT coronary artery calcium quantification: comparison with traditional filtered backprojection in vitro and in vivo. Radiology. 2014;270(2):387–93.
45. Morsbach F, Desbiolles L, Plass A, Leschka S, Schmidt B, Falk V, Alkadhi H, Stolzmann P. Stenosis quantification in coronary CT angiography: impact of an integrated circuit detector with iterative reconstruction. Invest Radiol. 2013;48(1):1–9.
46. Haubenreisser H, Fink C, Nance J, Sedlmair M, Schmidt B, Schoenberg S, Henzler T. Feasibility of slice width reduction for spiral cranial computed tomography using iterative image reconstruction. Eur J Radiol. 2014;83(6):964–9.
47. McCollough C, Leng S, Sunnegardh J, Vrieze T, Yu L, Lane J, Raupach R, Stierstorfer K, Flohr T. Spatial resolution improvement and dose reduction potential for inner ear CT imaging using a z-axis deconvolution technique. Med Phys. 2013;40(6):619041–9.
48. • Gordic S, Morsbach F, Schmidt B, Allmendinger T, Flohr T, Husarik D, Baumueller S, Raupach R, Stolzmann P, Leschka S, Frauenfelder T, Alkadhi H (2014) Ultralow-dose chest computed tomography for pulmonary nodule detection: first performance evaluation of single energy scanning with spectral shaping. Invest Radiol 49(7):465–73. *This study is the first report of the use of a novel scanning technique which adds a spectral shaping filter to the x-ray tube to improve the dose efficiency in non-contrast enhanced thorax examinations. The study found that this novel scanning technique, in conjunction with iterative reconstruction, enables ultra-low dose imaging, with doses in the range of a fraction of a millisievert (0.06 mSv) and stil maintaining image quality, sensitivity and diagnostic confidence.*
49. Gordic S, Desbiolles L, Stolzmann P, Gantner L, Leschka S, Husarik D, Alkadhi H. Advanced modelled iterative reconstruction for abdominal CT: qualitative and quantitative evaluation. Clin Radiol. 2014;69(12):e497–504.
50. Shuman W, Green D, Busey J, Kolokythas O, Mitsumori L, Koprowicz K, Thibault J, Hsieh J, Alessio A, Choi E, Kinahan P. Model-based iterative reconstruction versus adaptive statistical iterative reconstruction and filtered back projection in liver 64-MDCT: focal lesion detection, lesion conspicuity, and image noise. Am J Roentgenol AJR. 2013;200(5):1071–6.
51. Bruder H, Raupach R, Sunnegardh J, Sedlmair M, Stierstorfer K, Flohr T (2011) Adaptive iterative. In: Proceedings of SPIE Medical Imaging, San Diego, 2011.
52. Marin D, Boll DT, Mileto A, Nelson R. State of the art: dual-energy CT of the abdomen. Radiology. 2014;271(2):327–42.
53. Graser A, Johnson TR, Hecht EM, Becker CR, Leidecker C, Staehler M, Stief CG, Hildebrandt H, Godoy MC, Finn ME, Stepansky F, Reiser MF, Macari M. Dual-energy CT in patients suspected of having renal masses: can virtual nonenhanced images replace true non enhanced images? Radiology. 2009;252(2):433–40.
54. Flohr TG, McCollough CH, Bruder H, Petersilka M, Gruber K, Suss C, Grasruck M, Stierstorfer K, Krauss B, Raupach R, Primak AN, Kuttner A, Achenbach S, Becker C, Kopp A, Ohnesorge BM. First performance evaluation of a dual-source CT (DSCT) system. Eur Radiol. 2006;16:256–68.
55. Kaza R, Platt J, Cohan RH, Caoili E, Al-Hawary M, Wasnik A. Dual energy CT with single- and dual-source scanners: current applications in evaluating the genitourinary tract. Radiographics. 2012;32:353–69.
56. Johnson TR. Dual-energy CT: general principles. Am J Roentgenol AJR. 2012;199:S3–8.
57. • Primak AN, Ramirez-Giraldo JC, Eusemann CD, Schmidt B, Kantor B, Fletcher JG, McCollough CH. Dual-source dual-energy CT with additional tin filtration: Dose and image quality evaluation in phantoms and in vivo. Am J Roentgenol AJR. 2010;195(5):1164–74. *Furthermore, the study found that the increase in spectra separation allowed improved imaging in large patients by enabling scanning with a dual-energy pair in which the low tube potential operates at 100 kV and the high tube potential at 140 kV with the added spectra filtration.*
58. Schenzle J, Sommer W, Neumaier K, Michalski G, Lechel U, Nikolau K, Becker C, Reiser M, Johnson T. Dual-energy CT of the chest: how about the dose? Invest Radiol. 2010;45(6):347–53.
59. Purysko A, Primak A, Baker M, Obuchowski N, Remer E, John B, Herts B. Comparison of radiation dose and image quality from single-energy and dual-energy CT examinations in the same patients screened for hepatocellular carcinoma. Clin Radiol. 2014;69(12):e538–44.
60. Primak AN, Ramirez-Giraldo JC, Liu X, Yu L, McCollough CH. Improved dual-energy material discrimination for dual-source CT by means of additional spectral filtration. Med Phys. 2009;36(4):1359–69.
61. Newell JD, Fuld MK, Allmendinger T, Sieren JP, Chan K, Guo J, Hoffman EA. Very low-dose (0.15 mGy) chest CT protocols using the COPDGene 2 test object and a third-generation dual-source CT scanner with corresponding third-generation iterative reconstruction software. Invest Radiol. 2014;50(1):40–5.
62. Gnannt R, Winklehner A, Goetti R, Schmidt B, Kollias S, Alkadhi H. Low kilovoltage CT of the neck with 70 kVp: comparison with a standard protocol. AJNR Am J Neuroradiol. 2012;33(6):1014–9.
63. • Meyer M, Haubenreisser H, Schoepf UJ, Vliegenthart R, Leidecker C, Allmendiger T, Lehmann R, Sudarski S, Borggrefe M, Schoenberg SO, Henzler T. Closing in on the K edge: coronary CT angiography at 100, 80 and 70 kV-initial comparison of a second-versus a third-generation dual-source CT system. Radiology. 2014;273(2):373–82. *This study reported the use of an advanced x-ray tube which can maintain high-tube current (up to 1300 mA) at low tube potential of 70 kV. The study demonstrated that this technology enables coronary CT angiography examinations in nonobese adult patients at significantly reduced radiation dose levels of less than 0.5 mSv, and with reduced contrast medium amount (45 mL) while maintaining robust image quality.*
64. Christner JA, Zavaletta VA, Eusemann CD, Walz-Flannigan AI, McCollough CH. Dose reduction in helical CT: dynamically adjustable z-axis x-ray beam collimation. Am J Roentgenol AJR. 2010;194:W49–55.
65. Duan X, Wang J, Leng S, Schmidt B, Allmendinger T, Grant K, Flohr T, McCollough C. Electronic noise in CT detectors: impact on image noise and artifacts. Am J Roentgenol AJR. 2013;201(4):W626–32.
66. Morsbach F, Bickelhaupt S, Rätzer S, Schmidt B, Alkadhi H. Integrated circuit detector technology in abdominal CT: added value in obese patients. Am J Roentgenol. 2014;202(2):368–74.
67. Wang J, Kang T, Arepalli C, Barrett S, O'Connell T, Louis L, Nicolaou S, McLaughlin P. Half-dose non-contrast CT in the investigation of urolithiasis: image quality improvement with third-generation integrated circuit CT detectors. Abdom Imaging. 2014. doi:10.1007/s00261-014-0264-0.
68. Liu Y, Leng S, Michalak G, Vrieze T, Duan X, Qu M, Shiung M, McCollough C, Fletcher J. Reducing image noise in computed tomography (CT) colonography: effect of an integrated circuit CT detector. J Comput Assist Tomogr. 2014;38(3):398–403.
69. Fletcher JG, Grant KL, Fidler JL, Shiung M, Yu L, Wang J, Schmidt B, Allmendinger T, McCollough CH. Validation of

dual-source single-tube reconstruction as a method to obtain half-dose images to evaluate radiation dose and noise reduction: phantom and human assessment using CT colonography and sinogram-affirmed iterative reconstruction (SAFIRE). J Comput Assist Tomogr. 2012;36(5):560–9.
70. Morsbach F, Desbiolles L, Plass A, Leschka S, Schmidt B, Falk V, Alkadhi H, Stolzmann P. Stenosis quantification in coronary CT angiography: impact of an integrated circuit detector with iterative reconstruction. Invest Radiol. 2013;48(1):32–40.
71. Gassenmaier T, Petri N, Allmendinger T, Flohr T, Maintz D, Voelker W, Bley T. Next generation coronary CT angiography: in vitro evaluation of 27 coronary stents. Eur Radiol. 2014;24(11): 2953–61.
72. McCollough CH, Leng S, Sunnegardh J, Vrieze TJ, Yu L, Lane J, Raupach R, Stierstorfer K, Flohr TG. Spatial resolution improvement and dose reduction potential for inner ear CT imaging using a z-axis deconvolution technique. Med Phys. 2013;40(6):61904.
73. Meyer M, Haubenreisser H, Raupach R, Schmidt B, Lietzmann F, Leidecker C, Allmendiger T, Flohr T, Schad L, Schoenberg S, Henzler T. Initial results of a new generation dual source CT system using only an in-plane comb filter for ultra-high resolution temporal bone imaging. Eur Radiol. 2014;25(1):178–85.
74. Yu L, Liu X, Leng S, Kofler JM, Ramirez-Giraldo JC, Qu M, Christner J, Fletcher JG, McCollough CH. Radiation dose reduction in computed tomography: techniques and future perspective. Imaging Med. 2009;1(1):65–84.
75. Chen M, Shanbhaq S, Arai A. Submillisievert median radiation dose for coronary angiography with a second-generation 320-detector row CT scanner in 107 consecutive patients. Radiology. 2013;267(1):76–85.
76. Denison K, Katchalski T. Imaging: CT dose optimization technologies I partners in solutions imaging. Austin: American Association of Physicists in Medicine 56th annual meeting and exhibition; 2014.
77. Hausleiter J, Meyer T, Hermann F, Hadamitzky M, Krebs M, Gerber T, McCollough C, Martinoff S, Kastrati A, Schomig A, Achenbach S. Estimated radiation dose associated with cardiac CT angiography. JAMA. 2009;301(5):500–7.
78. Sun Z, Ng K. Diagnostic value of coronary CT angiography with prospective ECG-gating in the diagnosis of coronary artery disease: a systematic review and meta-analysis. Int J Cardiovasc Imaging. 2012;28(8):2109–19.
79. Achenbach S, Marwan M, Ropers D. Coronary computed tomography angiography with a consistent dose below 1 mSv using prospectively electrocardiogram-triggered high-pitch spiral acquisition. Eur Heart J. 2010;31(3):340–6.